THE JOURNAL OF BIOLOGICAL CHEMISTRY VOL. 286, NO. 49, pp. 42459–42469, December 9, 2011


# Pituitary Adenylate Cyclase-activating Peptide (PACAP) Recruits Low Voltage-activated T-type Calcium Influx under Acute Sympathetic Stimulation in Mouse Adrenal Chromaffin Cells*

Received for publication, August 3, 2011, and in revised form, October 17, 2011 Published, JBC Papers in Press, October 18, 2011, DOI 10.1074/jbc.M111.289389

**Jacqueline Hill, Shyue-An Chan, Barbara Kuri, and Corey Smith**[1]

*From the Department of Physiology and Biophysics, Case Western Reserve University, Cleveland, Ohio 44106*

**Background:** The acute stress secretagogue PACAP leads to catecholamine release, but the source of calcium necessary for secretion is unknown.
**Results:** PACAP stimulation increases LVA $Ca_v3.2$ influx in a PKC-dependent process.
**Conclusion:** PACAP-mediated acute sympathetic stress functionally recruits a pool of latent $Ca_v3.2$ channels to supply calcium for secretion.
**Significance:** Native sympathoadrenal stimulation elicits catecholamine release through a non-canonical mechanism.

**Low voltage-activated T-type $Ca_v3.2$ calcium channels are expressed in neurosecretory chromaffin cells of the adrenal medulla. Previous studies have shown that naïve adrenal chromaffin cells express a nominal $Ca_v3.2$-dependent conductance. However, $Ca_v3.2$ conductance is up-regulated following chronic hypoxia or long term exposure to cAMP analogs. Thus, although a link between chronic stressors and up-regulation of $Ca_v3.2$ exists, there are no reports testing the specific role of $Ca_v3.2$ channels in the acute sympathoadrenal stress response. In this study, we examined the effects of acute sympathetic stress on T-type $Ca_v3.2$ calcium influx in mouse chromaffin cells *in situ*. Pituitary adenylate cyclase-activating peptide (PACAP) is an excitatory neuroactive peptide transmitter released by the splanchnic nerve under elevated sympathetic activity to stimulate the adrenal medulla. PACAP stimulation did not evoke action potential firing in chromaffin cells but did cause a persistent subthreshold membrane depolarization that resulted in an immediate and robust $Ca^{2+}$-dependent catecholamine secretion. Moreover, PACAP-evoked secretion was sensitive to block by nickel chloride and was acutely inhibited by protein kinase C blockers. We utilized perforated patch electrophysiological recordings conducted in adrenal tissue slices to investigate the mechanism of PACAP-evoked calcium entry. We provide evidence that stimulation with exogenous PACAP and native neuronal stress stimulation both lead to a protein kinase C-mediated phosphodependent recruitment of a T-type $Ca_v3.2$ $Ca^{2+}$ influx. This in turn evokes catecholamine release during the acute sympathetic stress response.**

Adrenal medullary chromaffin cells are a primary output of the sympathetic nervous system, releasing catecholamines into the circulation (1). Sympathetic activity elicits catecholamine release through cholinergic synaptic input from the innervating splanchnic nerve. Splanchnic nerve-released acetylcholine binds to ionotropic receptors on chromaffin cells, triggering a sodium-based action potential that activates high voltage-activated calcium channels (2–4). Elevated intracellular calcium evokes an exocytic release of catecholamines (5). Under acute sympathetic stress, the splanchnic nerve exhibits elevated burst mode firing, driving greatly increased adrenal catecholamine release (6). However, sustained, elevated input leads to desensitization of chromaffin cells to cholinergic stimulation (7–10). This cholinergic desensitization occurs at the level of the nicotinic acetylcholine receptor as well as steps downstream in the secretion process (*i.e.* negative modulation of voltage-gated $Ca^{2+}$ channels) (1, 11, 12). Despite nicotinic desensitization, catecholamine secretion persists under sustained, elevated sympathetic stimulation (6, 13, 14). Thus, a non-cholinergic splanchnic-adrenal transmitter was predicted to elicit chromaffin cell catecholamine release under elevated stimulation (14). Previous work identified the peptidergic transmitter pituitary adenylate cyclase-activating peptide (PACAP)[2] as a likely candidate (15–17) to substitute for cholinergic adrenal stimulation under the sympathoadrenal stress response.

PACAP is a highly conserved member of the glucagon superfamily that also includes the closely related vasointestinal peptide. PACAP stimulation leads to an array of systemic functions, including regulation of cell differentiation (18, 19), cell division (20), and transcription of stress-associated genes (21). As a neurotransmitter, PACAP is present in the splanchnic nerve terminal and released preferentially under elevated sym-

* This work was supported, in whole or in part, by National Institutes of Health Grant T32 HL 07887. This work was also supported by American Heart Association Grant 10PRE4100002.

[1] To whom correspondence should be addressed: Dept. of Physiology and Biophysics, School of Medicine, Case Western Reserve University, 2109 Adelbert Rd., Cleveland, OH 44106. Tel.: 216-368-3487; Fax: 216-368-5582; E-mail: Corey.Smith@Case.Edu.

[2] The abbreviations used are: PACAP, pituitary adenylate cyclase-activating peptide; LVA, low voltage-activated; Epac, exchange protein activated by cAMP; HVA, high voltage-activated; 8-pCPT-2′-*O*-Me-cAMP, 8-(4-chlorophenylthio)-2′-*O*-methyladenosine 3′,5′-cyclic monophosphate; BBS, bicarbonate-buffered saline; $P_{V_m}$, PACAP potential; I-V, current-voltage; PMA, phorbol 12-myristate 13-acetate.

pathetic firing to elicit adrenal medullary catecholamine release (16, 22, 23). The predominant PACAP target receptor in the adrenal medulla is the high affinity $PAC_1$-R, a $G_s$-linked receptor that activates adenylate cyclase to increase cyclic adenosine monophosphate (cAMP) (24, 25). Recent studies have shown that PACAP stimulation activates the stimulatory exchange protein activated by cAMP (Epac) pathway through the elevation in cAMP (26, 27), triggering phospholipase C and a protein kinase C (PKC)-dependent subthreshold depolarization that is necessary for catecholamine release from chromaffin cells (16). PACAP-mediated exocytosis is independent of sodium-based action potentials (28) or nicotinic acetylcholine receptor function (29, 30), thus bypassing key sites of nicotinic secretory desensitization. However, the mode of calcium entry necessary for evoking exocytosis during acute PACAP stimulation remains unidentified. Because PACAP does not cause action potential firing, calcium entry through a high voltage-activated calcium channel seems unlikely during PACAP signaling. Furthermore, studies have shown that PACAP-evoked secretion is blocked by micromolar concentrations of nickel chloride as well as mibefradil, implicating the possible role of low voltage-activated T-type calcium channels in acute sympathetic stress (16).

Low voltage-activated T-type calcium channels ($Ca_v3.1$–$3.3$) have been shown to play a role in regulating the activity of excitable cells, and they are present in excitable tissues as diverse as neurons, neuroendocrine cells, and cardiac myocytes (31–38). T-type $Ca_v3.2$ channels are pharmacologically characterized by their selective block by micromolar concentrations of nickel chloride (39). Naïve adrenal chromaffin cells express little $Ca_v3.2$ channel conductance (40, 41). However, quantitative PCR has shown message for low voltage-activated (LVA) $Ca_v3.2$ T-type channel $\alpha$ subunit in the rat adrenal medulla (41). Recent studies have identified a role for T-type channels in chronic stress and have shown that expression is increased in response to chronic hypoxia or exposure to cAMP analogs (40–43), leading to the colloquialism that T-type channels are the "stress channels." Several factors predict that T-type $Ca^{2+}$ channels are a likely component of acute PACAP stimulation. Previous studies have shown that acute PACAP stimulation elicits a voltage-dependent influx of external calcium that is independent of the major high voltage-activated $Ca^{2+}$ channels (15, 44). Moreover, PACAP stimulation leads to an up-regulation of protein kinase C activity (16, 45, 46). PKC has been shown to positively modulate T-type channel conductance in other cell types (47). Therefore, we hypothesized that acute PACAP stimulation may functionally augment T-type conductance and in turn elicit catecholamine release. In this study, we provide data demonstrating that PACAP-evoked membrane depolarization was necessary but not sufficient to evoke catecholamine release. We further demonstrate that acute PACAP stimulation results in a PKC-dependent recruitment of T-type $Ca_v3.2$ influx and leads to subsequent catecholamine release.

## EXPERIMENTAL PROCEDURES

*Adrenal Slice Preparation*—Adult male C57BL/6 mice (4–8 weeks old) from The Jackson Laboratories (Bar Harbor, ME) were used in this study. Anesthesia and euthanasia protocols were approved by Case Western Reserve University's institutional animal care and use committee, a federal oversight body (Federal welfare assurance number A3145-01). Animals were deeply anesthetized by isoflurane (USP; Halocarbon Products Corp., River Ridge, NJ) inhalation and euthanized by decapitation. Adrenal glands were immediately excised and immersed in ice-cold low calcium bicarbonate-buffered saline (BBS) containing 140 mM NaCl, 2 mM KCl, 0.1 mM $CaCl_2$, 5 mM $MgCl_2$, 26 mM $NaHCO_3$, 10 mM glucose and bubbled with 95% $O_2$, 5% $CO_2$. All chemicals were from Fisher Scientific except $MgCl_2$ (Sigma-Aldrich). The osmolarity of the BBS solution was 320 mosmol·liter$^{-1}$. Glands were trimmed of excess fat and connective tissue and embedded in low melting temperature agarose (Lonza, Rockland, ME). Agarose was prepared by melting in low calcium BBS at 110 °C followed by equilibration in a 35 °C water bath. Immediately after embedding, glands and agarose were placed on ice to set. Gelled agarose was trimmed into 3–5-mm blocks, each containing a single adrenal gland. Agarose blocks were glued to a vibrotome sectioning stage (World Precision Instruments, Sarasota, FL). The stage was placed in a slicing chamber filled with ice-cold low calcium BBS that was continuously bubbled with 95% $O_2$, 5% $CO_2$. Adrenal glands were sectioned at 200 $\mu$m. Care was taken to preserve splanchnic innervation by cutting sections parallel to the long axis. Sections were collected and placed in a holding chamber containing low calcium BBS bubbled with 95% $O_2$, 5% $CO_2$ at 25 °C. Experiments were carried out within 7 h of slice preparation unless noted otherwise.

*Electrophysiology*—Tissue slices were constantly superfused during recordings with HEPES-buffered Ringer's solution containing 150 mM NaCl, 10 mM HEPES-H, 10 mM glucose, 2.8 mM $CaCl_2$, 2.8 mM KCl, 2 mM $MgCl_2$. The Ringer's solution was adjusted to pH 7.2 with NaOH, and osmolarity was adjusted with mannitol to 320 mosmol·liter$^{-1}$. Tissue slices were held in place in the recording chamber by placing a silver wire over the agarose perimeter of the adrenal slice. Patch pipettes were pulled from borosilicate glass (~1-$\mu$m tip diameter; 4–5-megaohm resistance). Pipette tips were dipped in molten dental wax and fire-polished with a microforge (Narishige, Tokyo, Japan). All recordings were conducted in the perforated patch configuration. Typically, cells one or two layers deep into the slice were chosen to avoid damaged cells and debris from the cut surface of the tissue slice. Data presented in this study were recorded from cells perforated to a series resistance of no more than 25 megaohms. Records with unstable series resistance were excluded from analysis.

For voltage clamp experiments, pipettes were filled with an internal patch solution containing 145 mM cesium glutamate, 10 mM HEPES-H, 8 mM NaCl, 0.5 mM tetraethylammonium chloride. The internal solution had a pH of 7.2 and osmolarity of 310 mosmol·liter$^{-1}$. Amphotericin B (Fisher Scientific) was prepared in DMSO (Acros Organics) as a 100× stock solution daily and diluted into the internal solution to a final concentration of 0.53 mM. The liquid junction potential between HEPES Ringer's solution and the internal solution was measured to be 17.8 mV through an agar bridge as described (48). Junction potentials and series resistance compensation were adjusted in

all records accordingly. For current clamp experiments, pipettes were filled with an internal solution containing 145 mM potassium glutamate, 10 mM HEPES-H, 8 mM NaCl, 1 mM $MgCl_2$, 0.53 mM amphotericin B; pH was adjusted to 7.2, and osmolarity was adjusted to 310 mosmol·liter$^{-1}$. Electrophysiological records were filtered at 10 kHz and digitized at 20 kHz using an EPC-9 amplifier under the control of Pulse software (version 8.8; HEKA Electronik, Bellmore, NY). All electrophysiological data were analyzed using Igor Pro software (WaveMetrics Inc., Lake Oswego, OR).

The protocol used to construct and collect current-voltage (I-V) plots was as follows. Cells were held at −80 mV, and 30 depolarizing steps from −100 to +45 mV in 5-mV increments with each potential pulse lasting 50 ms and an intersweep interval of 15 s were delivered. To isolate $Ni^{2+}$-sensitive current from total calcium current, the I-V protocol was delivered twice, once in normal extracellular HEPES solution and then again in a HEPES solution supplemented with 50 μm Ni(II) chloride hexahydrate (Sigma-Aldrich). A microperfusion system (Warner Instruments, Hamden, CT) was used for local rapid delivery of pharmacological agents (see text) as well as nickel chloride-containing Ringer's solutions during recordings.

*Amperometry*—Carbon fiber electrodes of 5 μm diameter (ALA Scientific Instruments, Westbury, NY) were used for detection of catecholamine secretion in chromaffin cells *in situ* (49). Cells were chosen based on their relative orientation with the capillary secretory pole available for the carbon fiber electrode. Carbon fibers were placed as close to a cell as possible without distorting the cell membrane. During amperometric recordings, a +650-mV charge was placed on the fiber through a dedicated VA-10X amperometry amplifier (ALA Scientific Instruments). Oxidative current was acquired through the VA-10X, prefiltered at 1.3 kHz, and digitized at 20 kHz through an ITC-1600 digital to analog convertor (InstruTECH, Bellmore, NY). Data were acquired and analyzed through a custom-written macro running under Igor Pro.

*Bipolar Nerve Stimulation*—The adrenal splanchnic nerve was excited by a bipolar stimulator (FHC, Inc., Bowdoin, ME) designed with two platinum electrodes spaced 250 μm apart. The electrodes were connected to an ISO-Stim 01-D stimulator (NPI Electronic, Tamm, Germany). The ISO-Stim 01-D was controlled by Pulse-issued transistor-transistor logic triggers issued through the EPC-9 patch amplifier. To identify functionally innervated chromaffin cells, the bipolar stimulator was paced at a low frequency (0.05 Hz), and an amperometric carbon fiber was used to probe for responding medullary cells. Synaptic coupling was further confirmed by blocking nicotinic receptors with hexamethonium. Under "Low Hz" stimulation, the splanchnic nerve was stimulated for 60 pulses at a frequency of 0.2 Hz. Under "High Hz" stimulation, the nerve was stimulated with four bursts of 15 pulses at 2 Hz frequency with an interburst interval of 15 s. Stimuli were delivered at a constant voltage of 35 V for a 10 μs duration. Quantified pooled data were determined from base line-subtracted, integrated amperometric currents at the 120 s time point.

*Quantitative PCR*—RNA was isolated by a TRIzol extraction and normalized to a concentration standard of 500 ng/μl per reaction. RT-quantitative PCR was performed according to the manufacturer's specifications (Applied Biosystems, Carlsbad, CA) on the StepOnePlus Real-Time PCR System (Applied Biosystems). Reverse transcription was performed using the TaqMan RNA-to-$C_T$ 1-step kit. Real time primers were purchased from Applied Biosystems ($Ca_v$3.1, Mm01299131_m1; $Ca_v$3.2, Mm00445369_m1; $Ca_v$3.3, Mm00445369_m1; GAPDH, Mm99999915_g1).

*Immunohistochemistry*—Mice were deeply anesthetized and perfused through left ventricle catheterization. The perfusate consisted first of phosphate-buffered saline and was quickly followed by phosphate-buffered 10% formalin. Glands were removed and postfixed for 1 h in the same fixative. The glands were then embedded in OCT compound (Ted Pella, Inc., Redding, CA), cryosectioned into 16 μm sections, and mounted on slides. To probe for tyrosine hydroxylase and $Ca_v$3.2 T-type $Ca^{2+}$ channel expression, the adrenal sections were washed with PBS and blocked with a solution of 4% donkey serum in PBS containing 0.15% Triton X-100 for 60 min at room temperature. The sections were incubated with sheep anti-mouse tyrosine hydroxylase IgG (1:500; Millipore; catalog number P07101) and rabbit anti-mouse $Ca_v$3.2 IgG (1:100; Alomone Labs, Jerusalem, Israel; catalog number ACC-025) overnight at 4 °C. The sections were washed with PBS and incubated with donkey anti-sheep Alexa Fluor 488 (1:100) and donkey anti-rabbit Alexa Fluor 594 (1:100; Invitrogen) for 2 h at room temperature. Sections were washed with PBS and mounted with Immu-Mount (Thermo Scientific, Pittsburgh, PA). Fluorescence signals were visualized on an Olympus IX81 microscope at 40× magnification and acquired by the SlideBook imaging system (Denver, CO) using a Q Imaging Systems charge-coupled device camera (Surrey, British Columbia, Canada).

*Statistical Analysis*—The specific analysis used for quantification of the data in each figure is included in the text and/or figure legends. Student's *t* test was utilized to assess significance in data sets where control and treatment conditions were from the same cell. In data sets where multiple experimental data sets were compared with control data from different cells, a one-way analysis of variance test was utilized. Statistical barriers for either condition are indicated in the legends.

## RESULTS

The peptide transmitter PACAP is stored in terminals of the splanchnic nerve and released onto adrenal chromaffin cells under elevated sympathetic firing to elicit catecholamine secretion (14–16). Here we report the results of a study designed to test the mechanism of the acute PACAP secretory response in adrenal chromaffin cells. We combined immunostaining with *in situ* electrophysiological, electrochemical, and native neuronal stimulation of adrenal medullary chromaffin cells to investigate the mode of PACAP-evoked $Ca^{2+}$ influx and secretion. All experiments were performed in adrenal tissue slices, and electrical recordings were performed in the perforated patch configuration to preserve as much as possible the native signaling context of the chromaffin cell secretory apparatus (50, 51).

*PACAP Evokes Subthreshold Membrane Depolarization and Nickel-sensitive Catecholamine Release*—Previous studies from our laboratory and others have shown that PACAP is a strong

secretagogue for catecholamine release, but PACAP stimulation does not elicit action potentials in chromaffin cells. However, PACAP does cause a subthreshold depolarization that in turn elicits influx of external $Ca^{2+}$ (16, 52). Studies have addressed the effect of PACAP stimulation on voltage-gated calcium current and yielded a variety of results showing either depression or augmentation of current through conventional high voltage-activated (HVA) channels depending on the channel isotype or the time frame studied (53–55). However, little is known of how acute PACAP stimulation elicits $Ca^{2+}$ influx in response to the evoked subthreshold depolarization. To discern which calcium channel isotype may be involved in acute PACAP stimulation, we initially assessed the effect of PACAP on two key electrophysiological properties, membrane potential and action potential-evoked calcium influx. An example recording demonstrating the subthreshold depolarization evoked by PACAP stimulation is provided (Fig. 1*A*, *panel i*). A cell was held in a perforated patch current clamp and stimulated by puffing on 1 $\mu$M PACAP. In this example recording, the cell membrane potential depolarized by 17 mV to an average value of −53 mV (referred to in this study as the "PACAP potential" ("$P_{V_m}$")). Thus, although resulting in a membrane depolarization, PACAP stimulation did not elicit an action potential.

We considered the potential role for PACAP as a modulator of canonical action potential-based excitation. The shape of the action potential has been shown to specifically activate certain HVA $Ca^{2+}$ channels to a greater degree than others (3). We confirmed that exogenous PACAP had no significant effect on high voltage-activated $Ca^{2+}$ influx evoked by action potential stimulation. In this set of recordings, cells were held in voltage clamp and stimulated with a native action potential voltage template (Fig. 1*A*, *panel ii*) prior to (*dotted line*) and after exposure to PACAP (*solid line*). Mean $Ca^{2+}$ currents recorded under voltage clamp action potential stimulation as well as the mean PACAP-evoked membrane depolarization were pooled and are reported in Fig. 1*B*. These results suggest that the calcium influx observed during PACAP-dependent stimulation was not due to $Ca^{2+}$ influx by the canonical action potential-activated HVA $Ca^{2+}$ channels. However, the subthreshold depolarization would allow for activation of LVA calcium channels, including members of the T-type calcium channel family. Thus, we assessed whether PACAP-evoked secretion is sensitive to blockers of T-type calcium channels. Representative recordings are provided in Fig. 1*C*, *panel i*, to demonstrate the secretagogue effect of acute PACAP stimulation. PACAP was focally perfused onto a single chromaffin cell, and a robust integrated amperometric current was recorded (140.3 ± 46.5 picocoulombs; $n = 10$). Secretion was not observed in the presence of the T-type blocker $NiCl_2$ as shown in Fig. 1*C*, *panel ii* (6.8 ± 5.6 picocoulombs; $n = 10$).

*T-type $Ca_v3.2$ Calcium Channel Expression and Conductance in Chromaffin Cells*—Acute PACAP-evoked $Ca^{2+}$ influx has been shown to be blocked by extracellular $Zn^{2+}$ (15). Albeit less sensitive or specific than block by $Ni^{2+}$ (36), $Zn^{2+}$ block is consistent with a T-type $Ca^{2+}$ influx. T-type channels are characterized by their ability to be activated under modest depolarization. T-type channels have been shown previously to play a

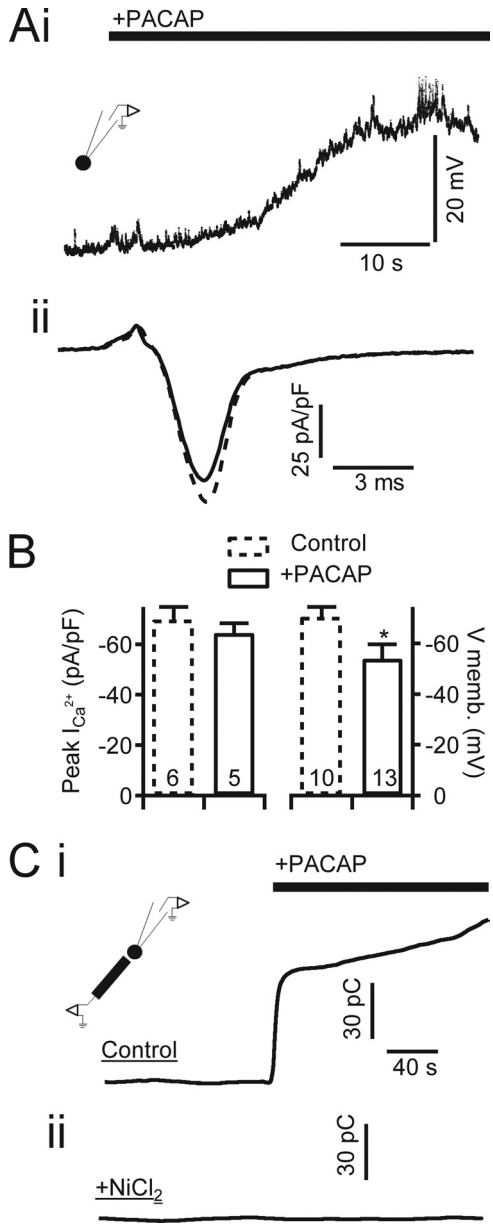


FIGURE 1. **PACAP evokes membrane depolarization and nickel-sensitive catecholamine release.** *A*, *panel i*, a chromaffin cell was held in perforated patch configuration, and membrane potential was measured under current clamp. Focal perfusion of PACAP (1 $\mu$M) is indicated by the *bar*. The *inset icon* indicates the patch clamp recording condition. *A*, *panel ii*, representative current recorded during perforated patch voltage clamp recordings of chromaffin cells stimulated with an action potential voltage template in control cells (*dash line*) or PACAP-treated cells (*solid line*). *B*, data quantified from pooled experiments such as in *A* show that PACAP stimulation does not significantly alter peak $Ca^{2+}$ influx during the action potential but does cause a significant membrane depolarization to approximately −53 mV ($P_{V_m}$). Data are plotted as mean value, with *error bars* representing S.E. * indicates significance at $p < 0.02$ by Student's *t* test; sample size is indicated by *numbers* at the *base* of each category *bar*. *C*, carbon fiber amperometry was utilized to measure catecholamine release under PACAP stimulation. Total catecholamine release for each condition was determined by integrating the time-resolved amperometric traces. The *inset icon* indicates the amperometric recording condition. *Panel i*, in untreated "*Control*" cells, focal perfusion of 1 $\mu$M PACAP elicits a robust catecholamine release indicated by a rapidly rising integrated amperometric current. *Panel ii*, perfusion in Ringer's solution supplemented with 50 $\mu$M $NiCl_2$ effectively blocks catecholamine release under PACAP stimulation. *pF*, picofarads; *memb.*, membrane; *pC*, picocoulombs.

role in adrenal medullary adaptation to stress with their expression increased in response to stressors (40, 42, 43). However, these and other studies report little to no T-type conductance in unstressed naïve isolated rat adrenal chromaffin cells (40, 41), isolated mouse cells (2), or even in mouse adrenal tissue slices (2, 3), a finding inconsistent with a putative involvement in the acute PACAP secretory response. We conducted reverse transcription-quantitative PCR to measure message for $Ca_v3.1$, $Ca_v3.2$, and $Ca_v3.3$ T-type channels in the unstressed adrenal medulla (GAPDH served as a positive control). The resulting amplification curves demonstrated equivalent message for all T-type channel isoforms ($C_t$ = 31, 32, and 32, respectively). Of these, only $Ca_v3.2$ channels exhibit high affinity block by $NiCl_2$ (56), identifying it as the most likely molecular isoform involved in PACAP adrenal stimulation (36, 39, 57). Thus, we conducted *in situ* immunofluorescent staining for $Ca_v3.2$ in adrenal slices. Example images are provided in Fig. 2*A* and show that there was a high degree of immunoreactivity for $Ca_v3.2$ that co-localized to cells showing positive staining for the neuroendocrine cell marker tyrosine hydroxylase. Additionally, PACAP staining was peripheral to $Ca_v3.2$-positive cells, consistent with PACAP-containing splanchnic terminals innervating the $Ca_v3.2$-positive chromaffin cells. Thus, our data support that in adult mouse adrenal medulla $Ca_v3.2$ message and protein are present in naïve chromaffin cells.

As demonstrated in Fig. 1, PACAP did not lead to a discrete excitation event such as an action potential; rather, the depolarization was sustained. This condition dictates that any $Ca^{2+}$ influx through a $Ca_v3.2$ channel would be due to a non-inactivating, persistent window current. We tested for a PACAP-evoked window current by electrophysiological perforated voltage clamp recordings conducted in adrenal tissue slices. We utilized a voltage clamp protocol in which a chromaffin cell was held at a $P_{V_m}$ of −53 mV (Fig. 2*B*) and treated with PACAP-containing or PACAP- and $NiCl_2$-containing Ringer's solution. The representative record shown in this panel exhibits a PACAP-evoked increase in inward conductance, and this conductance was blocked by 50 $\mu$M $NiCl_2$. The magnitude and further pharmacologic characterization of the PACAP-evoked window current follow in later figures.

$Ca_v3.2$ channels exhibit a slowly deactivating tail current that has been used as a diagnostic tool to quantify the emergence of T-type calcium channel conductance (43). We set out to quantify tail current kinetics at potentials relevant to PACAP stimulation to provide positive identification for the emergence of T-type calcium channels. The voltage protocol was to depolarize cells to +20 mV to fully activate all voltage-gated $Ca^{2+}$ channels and then step to $P_{V_m}$. We then fit the tail current with a double exponential decay function and anticipated a greater amplitude for the slow component as reported in the literature (43). However, when we conducted this analysis, we noted that the PACAP-treated cells exhibited a significant non-inactivating conductance (Fig. 2*C*) as would be expected from the augmentation of an LVA T-type window current (39, 40). This window current obscured the kinetics of the tail currents, making the intended analysis impossible. However, its presence led to a plausible mechanism explaining the observed PACAP-evoked, $Ni^{2+}$-sensitive inward conductance shown in Fig. 2*B*. It

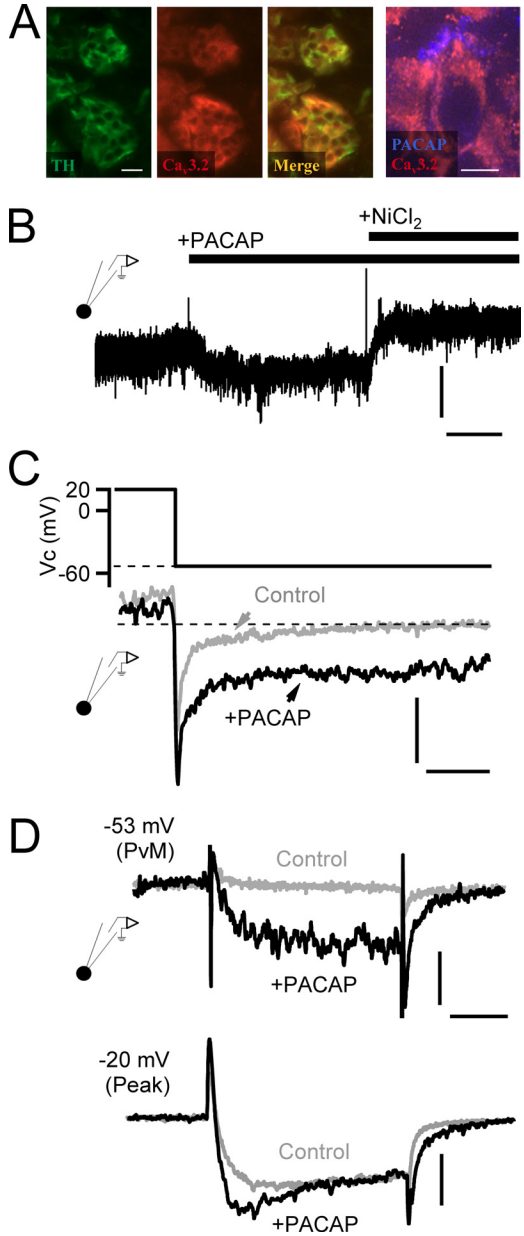


FIGURE 2. **PACAP facilitates nickel-sensitive current at negative potentials.** *A*, immunostaining for tyrosine hydroxylase (*TH*; *green* panel), a marker for catecholamine-secreting adrenal chromaffin cells, and $Ca_v3.2$ T-type calcium channels (*red* panel) are shown. The merge overlay ("*Merge*") indicates that both signals are present in the same cells of the adrenal medulla (*scale bar*, 50 $\mu$m). The panel to the *right* shows staining for PACAP and $Ca_v3.2$ at a higher resolution (*scale bar*, 10 $\mu$m) and shows a peripheral staining for PACAP surrounding the $Ca_v3.2$-positive chromaffin cell. *B*, a chromaffin cell was held at −53-mV command potential to match $P_{V_m}$, and the membrane current was measured. Puffing of exogenous PACAP (1 $\mu$M) elicited a sustained inward current. *Vertical scale bar*, 6 pA/picofarad; *horizontal scale bar*, 30 s. The PACAP-evoked current was blocked by the additional perfusion with 50 $\mu$M $NiCl_2$. *C*, a protocol was designed to assess PACAP-dependent effects on $Ca^{2+}$ tail currents. Representative records are provided, demonstrating that a depolarization to 20 mV and return to $P_{V_m}$ resulted in a specific enhancement of a non-inactivating window current in PACAP-treated cells. *Vertical scale bar*, 6 pA/picofarad; *horizontal scale bar*, 10 ms. *D*, voltage clamp depolarization from −80-mV holding potential to $P_{V_m}$ (−53 mV) elicits both a specific augmentation of inward current and a slower deactivating tail current specifically after stimulation with exogenous PACAP (10 $\mu$M). Depolarization to −20 mV ("*Peak*") to maximally activate all voltage-gated calcium channels elicits a specific emergence of a rapidly activating component as well as a slowly deactivating tail current after PACAP stimulation. *Horizontal scale bar*, 15 ms; *vertical scale bar*: −53 mV, 4 pA/picofarad; −20 mV, 5 pA/picofarad.

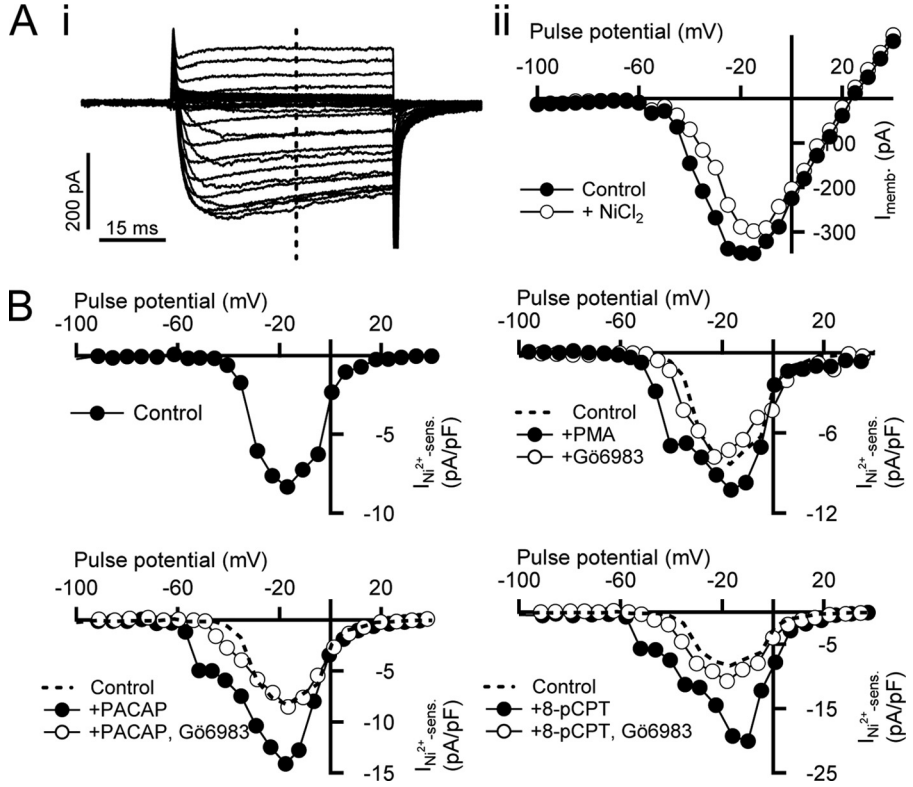


FIGURE 3. **PACAP-evoked facilitation of nickel-sensitive current is reversed by PKC inhibition.** *A*, a cell was held in perforated voltage clamp *in situ* and stimulated with an I-V protocol as described in the text. Steady state current was measured (*panel i*, *vertical dotted line*) and plotted against step potential in control Ringer's solution conditions (*panel ii*, ●) and after perfusion with Ringer's solution supplemented with 50 $\mu$M $NiCl_2$ (*panel ii*, ○). *B*, *top left* plot, a subtraction current of the data presented in *A* demonstrates the $Ni^{2+}$-sensitive current component. The same protocol as summarized in *A* was repeated in cells either treated with 1 $\mu$M exogenous PACAP (*bottom left* plot, ●) or PACAP and 100 nM Gö6983 (*bottom left* plot, ○). $Ni^{2+}$-sensitive (*sens.*) subtraction currents are plotted for each condition. For comparison, the nickel-sensitive current measured in control cells (*top left plot*) is replotted as a *dotted line*. The same protocol as summarized in *A* was repeated in 100 nM PMA (*top right* plot, ●) and Gö6983 (*top right* plot, ○)-treated cells (*top right* plot). Conditions are the same as in the other plots except the pharmacological conditions are 100 $\mu$M 8-pCPT-2′-*O*-Me-cAMP (*8-cPCT*; *bottom right* plot, ●) or 8-pCPT-2′-*O*-Me-cAMP and Gö6983 (*bottom right* plot, ○).

is possible that PACAP excitation leads to the functional recruitment of a non-inactivating LVA T-type $Ca_v3.2$ window current necessary to supply the calcium needed for prolonged PACAP-evoked secretion. We further studied the effect of PACAP on evoked calcium current. We held cells at −80 mV and delivered voltage steps to the PACAP-evoked resting potential ($P_{V_m}$, −53 mV) or the potential at which peak $Ca^{2+}$ influx is evoked (−20 mV). This protocol was delivered to naïve control cells or to cells acutely treated with PACAP (perfusion with 1 $\mu$M PACAP for 5 min). Representative recordings for each condition are provided in Fig. 2*D*. Stepping naïve cells to $P_{V_m}$ had little effect on inward conductance, whereas cells pretreated with exogenous PACAP exhibited a greatly facilitated inward current that was followed by a slowly deactivating tail current upon repolarization to −80 mV. Moreover, stepping the PACAP-treated cells to −20 mV to evoke maximal activation of all voltage-operated calcium conductances resulted in an increased peak conductance as well as the persistent slowly inactivating tail current compared with control cells. Both these characteristics are consistent with a $Ca_v3.2$ channel conductance (39, 43).

*PACAP Facilitates Nickel-sensitive Current*—Emergence of an LVA calcium conductance under PACAP stimulation should be readily evident as a negatively activating component in current-voltage plots. We assessed the effect of nickel chloride on current-voltage relationships in naïve and PACAP-treated chromaffin cells. Cells were held in the perforated patch configuration and voltage-clamped at a holding potential of −80 mV. Cells were then subjected to 50-ms voltage steps at 5-mV increments from −100 mV to a peak potential of +45 mV. The majority of recordings were conducted in normal BBS as described above to maintain native $Na^+$-dependent metabolic processes such as $Na^+/Ca^{2+}$, $Na^+/K^+$, and $Na^+/H^+$ exchange over the long duration of the recordings. However, we also conducted some recordings in the presence of tetrodotoxin (300 nM) to totally isolate $Ca^{2+}$ influx. Example evoked raw current traces from this protocol are provided in Fig. 3*A*, *panel i*. Throughout the study, the protocol was first delivered in standard Ringer's solutions and then repeated in a Ringer's solution supplemented with 50 $\mu$M $NiCl_2$ to allow for trace subtraction and isolation of the $Ni^{2+}$-sensitive component. As demonstrated in Fig. 1, PACAP-evoked catecholamine secretion did not result from a discrete signaling event such as the firing of an action potential. Rather, PACAP stimulation resulted in a subthreshold membrane depolarization that allowed a tonic window current to bring $Ca^{2+}$ into the cell to support exocytosis as shown in Fig. 2. Thus, we measured $Ca^{2+}$ flux after initial current inactivation (25 ms). An example paired I-V experiment conducted in a single cell is provided in Fig. 3*A*, *panel i* (*dotted line* at the 25-ms time point). In this

example experiment, only a modest portion of calcium current was blocked by $NiCl_2$ (Fig. 3*A*, *panel ii*). Subtraction-isolation of the $Ni^{2+}$-sensitive component revealed a more positive activation potential than that expected for LVA T-type channels (Fig. 3*B*, *upper left*) and may represent a partial $Ni^{2+}$ block of R-type channels (39). Indeed, R-type channels have been shown to contribute a significant conductance in naïve adrenal tissue slices (2). If PACAP-evoked calcium entry occurs through LVA nickel-sensitive calcium channels, then we would expect to see a facilitation of voltage-gated calcium current at more negative membrane potentials in the presence of PACAP. Indeed, we found that PACAP facilitated nickel-sensitive current at negative voltages and produced a low voltage-activated "shoulder" indicative of LVA T-type channels (Fig. 3*B*, *lower left*) (41–43, 58, 59). Thus, our data suggest that PACAP stimulation augments a $Ca^{2+}$ influx through an LVA conductance.

*PACAP Facilitates $Ni^{2+}$-sensitive Current in PKC-dependent Manner*—Previous studies have shown a dependence of PACAP-evoked secretion on the activation of PKC (16, 45, 60). We set out to determine whether the PACAP-mediated emergence of the LVA $Ca^{2+}$ influx is sensitive to PKC inhibition. We again repeated the above I-V/$Ni^{2+}$ block assay in the presence of PACAP and the conventional PKC blocker Gö6983 (100 nM), a compound shown previously to effectively block PACAP-mediated secretion in this preparation and at this concentration (16). As demonstrated in Fig. 3*B*, *lower left*, Gö6983 effectively decreased the magnitude of $Ni^{2+}$-sensitive current, shifted the activation potential back toward the positive, and eliminated the PACAP-induced low voltage shoulder to match the I-V measured in naïve cells (*dotted line*). Next, we repeated the same protocol in the presence of the PKC activator phorbol 12-myristate 13-acetate (PMA). Similar to PACAP-stimulated cells, we observed a low voltage shoulder indicative of LVA T-type channels (Fig. 3*B*, *upper right*). We next assessed the role of endogenous PKC activity by repeating the I-V/$Ni^{2+}$ block assay by treating cells with Gö6983 (Fig. 3*B*, *upper right*). Treatment of cells with Gö6983 alone did not alter LVA conductance nor did it decrease nickel-sensitive current, suggesting that endogenous PKC activity is not crucial for establishing basal LVA current levels.

PACAP receptor activation of PKC signaling includes a cAMP-mediated activation of Epac (26, 27, 61) through phospholipase C activation (16). We tested whether this signaling path regulates PACAP augmentation of LVA $Ca^{2+}$ influx. No specific Epac inhibitors are yet available; rather, we turned to the specific Epac activator 8-pCPT-2′-*O*-Me-cAMP (100 $\mu$M) (62, 63). As demonstrated in Fig. 3*B*, *lower right*, 8-pCPT-2′-*O*-Me-cAMP treatment quantitatively mimicked the effect of PACAP treatment, facilitating the nickel-sensitive $Ca^{2+}$ conductance and shifting its activation potential to the negative. Moreover, co-treating the slices with 8-pCPT-2′-*O*-Me-cAMP and Gö6983 had the same effect as co-treatment with PACAP and Gö6983, reversing the facilitation and causing a shift in activation potential to again match that measured in control cells (*dotted line*). Taken together, these data demonstrate that PACAP excitation evokes an LVA $Ca^{2+}$ conductance that is both electrophysiologically consistent with $Ca_v3.2$ channel

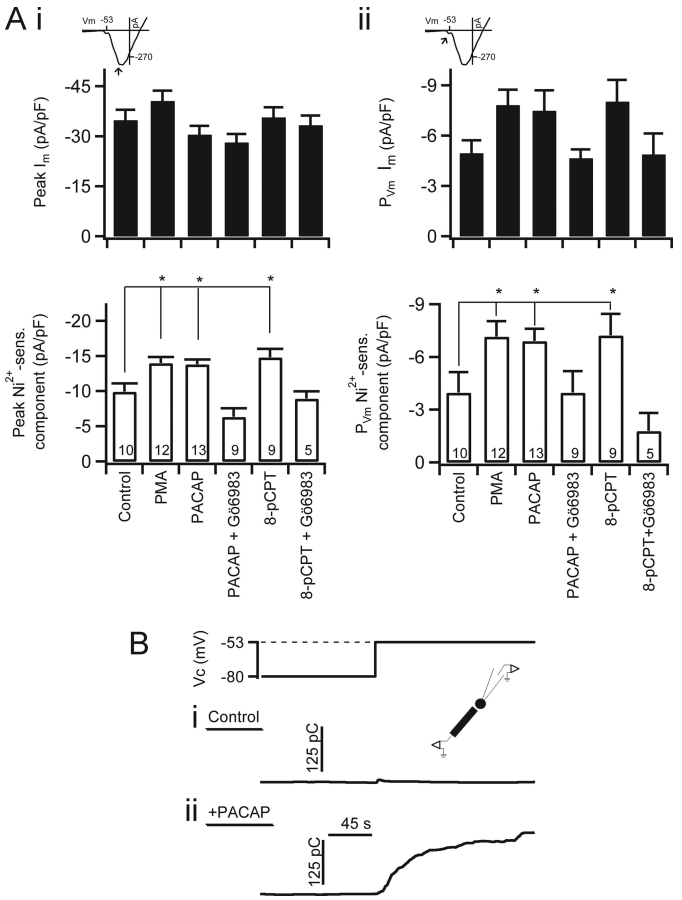


FIGURE 4. **PACAP, PMA, and 8-pCPT-2′-*O*-Me-cAMP facilitate nickel-sensitive current.** *A*, *inset icons* indicate the point in the I-V curve where current magnitudes were measured. Category plots on the *left* (*panel i*) represent peak inward values, whereas those on the *right* (*panel ii*) represent $P_{V_m}$ values. Data were pooled from experimental conditions as represented in Fig. 3 and are plotted as mean value with *error bars* representing S.E. *Upper* category plot, no significant difference was found in total peak current for any condition *versus* control. No significant difference was found in any pharmacological condition with respect to control peak $Ca^{2+}$ current. *Lower* category plot, nickel-sensitive $Ca^{2+}$ influx was determined as the difference between currents measured in normal Ringer's and $Ni^{2+}$-containing Ringer's solutions. * indicates $p \leq 0.05$ determined by one-way analysis of variance. Sample size is indicated by the *number* at the *base* of each category *bar*. *8-cPCT*, 8-pCPT-2′-*O*-Me-cAMP. *B*, the *inset icon* indicates a combined voltage clamp and amperometry experimental configuration. A voltage protocol was designed to test catecholamine secretion at $P_{V_m}$. A cell was held in perforated patch configuration and stepped from the holding potential of −80 to −53 mV. The resulting integrated amperometric current is shown for a control, naïve cell (*panel i*, *Control*) and for a cell that had been treated for 5 min with 1 $\mu$M exogenous PACAP by focal perfusion (*panel ii*, *+PACAP*). The increased integrated amperometric current in the *lower* trace indicates a sustained and robust catecholamine secretion in the PACAP-treated cell. *pF*, picofarad; *sens.*, sensitive; *pC*, picocoulombs.

activation and pharmacologically consistent with PACAP-evoked catecholamine release.

We repeated the experiments presented in Fig. 3 and pooled the measured peak total inward current (Fig. 4*A*, *panels i* and *ii*, *top filled* category *bars*) and the $Ni^{2+}$-sensitive component (Fig. 4*A*, *panels i* and *ii*, *lower hollow* category *bars*). The *insets* indicate with an *arrow* where calcium current was measured for each collimated plot pairing. These data show that treatment of chromaffin cells with either PACAP or PMA did not significantly change total peak calcium current density compared with control conditions nor did co-treatment with Gö6983,

8-pCPT-2′-*O*-Me-cAMP, or 8-pCPT-2′-*O*-Me-cAMP and Gö6983 (Fig. 4*A*, *panel i*, *upper* plot). This is an expected result in that none of these treatments were anticipated to have a significant effect on HVA $Ca^{2+}$ channels, which are the major component of the peak current (*inset*, *arrow*). However, when just the $Ni^{2+}$-sensitive component was separated out by subtraction as demonstrated in Fig. 3*B*, PACAP, PMA, and 8-pCPT-2′-*O*-Me-cAMP treatments significantly increased inward current at the peak potential, and block of PKC with Gö6983 reversed the effect (Fig. 4*A*, *panel i*, *lower* plot). This result is consistent with a specific effect on $Ni^{2+}$-sensitive $Ca_v3.2$ channels. Thus, PACAP-dependent facilitation of the LVA calcium current exhibits a pharmacological profile similar to that demonstrated for PACAP-evoked catecholamine release, including sensitivity to inhibition of PKC and an upstream activation by 8-pCPT-2′-*O*-Me-cAMP.

*Majority of Current at $P_{Vm}$ Is Sensitive to PACAP Modulation*—Chromaffin cells have a resting membrane potential of approximately −70 mV (3, 64). In Fig. 1, we showed that PACAP stimulation led to a subthreshold membrane depolarization of 17 mV to a potential of −53 mV. Thus, this −53-mV potential represents the effective voltage under which PACAP elicits catecholamine secretion. We therefore tested whether PACAP potentiates nickel-sensitive conductances at this $P_{V_m}$. As in Fig. 3, we analyzed total $Ca^{2+}$ influx during the I-V protocol and subtracted the remaining currents after superfusion with a $Ni^{2+}$-containing Ringer's solution. We first examined the effect of PACAP on total calcium current at $P_{V_m}$. Although there was a strong trend, neither PACAP nor PMA significantly increased total calcium current at $P_{V_m}$ at a statistical barrier of 0.02 (Fig. 4*A*, *panel ii*, *upper* plot). Similarly, when cells were treated with PACAP and Gö6983, total current at $P_{V_m}$ was not significantly affected. Finally, 8-pCPT-2′-*O*-Me-cAMP treatment also did not significantly change total calcium current at $P_{V_m}$. Although a trend mirroring the $Ni^{2+}$-sensitive current did emerge in the total current categories at $P_{V_m}$, the failure to reach significance in any data set was not due to a sample size effect. Sample size analysis was performed (65), and the sample size was shown to be sufficient for statistical evaluation. Rather, the total current was expected to be similar to the $Ni^{2+}$-sensitive component in that conductance at $P_{V_m}$ was dominated by LVA $Ca^{2+}$ channel conductance. However, the total current also represents various other conductances, including low probability opening of HVA calcium channels and voltage-gated $Na^+$ channels as well as electrogenic pumps and exchangers (*i.e.* $Na^+/Ca^{2+}$ and $Na^+/H^+$ exchangers). Thus, the observed trend in total current was expected, whereas significant differences with respect to the control condition were not necessarily expected.

Next, we wanted to determine whether PACAP also facilitates the nickel-sensitive current at $P_{V_m}$ again because this is the most relevant membrane potential for PACAP excitation and reflects the physiological condition under which PACAP evokes catecholamine secretion. Chromaffin cells were treated with PACAP as described above. PACAP treatment increased current at $P_{V_m}$ by 2-fold (Fig. 4*A*, *panel ii*, *lower* plot). Again, the PACAP-mediated facilitation at $P_{V_m}$ was mimicked by treatment with 8-pCPT-2′-*O*-Me-cAMP and PMA, and co-treatment with 8-pCPT-2′-*O*-Me-cAMP and Gö6983 reversed both of these effects. This result led to a testable prediction that voltage clamp to $P_{V_m}$ should only elicit catecholamine release in PACAP-treated cells (*lower* plot), whereas in untreated, naïve chromaffin cells, depolarization to $P_{V_m}$ is not sufficient to elicit catecholamine secretion. The experiment is outlined in Fig. 4*B*. Voltage clamp of naïve cells at $P_{V_m}$ did not cause significant catecholamine exocytosis (Fig. 4*B*, *panel i*) (23.6 ± 9.1 picocoulombs; $n = 6$). However, the same electrical step depolarization elicited a robust catecholamine release in cells acutely treated with PACAP (Fig. 4*B*, *panel ii*) (113.0 ± 24.9 picocoulombs; $n = 9$). This result indicates that in addition to membrane depolarization PACAP-mediated facilitation of LVA $Ca^{2+}$ influx is required for evoked catecholamine secretion.

*In Situ Stimulation of Splanchnic Nerve Facilitates $Ni^{2+}$-sensitive Current*—We have so far shown that nickel-sensitive current in naïve chromaffin cells was modest and followed an activation potential characteristic of HVA channels. We have shown that treatment with exogenous PACAP significantly facilitated an LVA, $Ni^{2+}$-sensitive conductance. We next set out to test whether this process is indeed associated with native sympathetic adrenal excitation and whether it occurs selectively under elevated neuronal stimulation. To address this question, we turned to a bipolar stimulation technique to directly excite the innervating splanchnic nerve (16). The experimental setup is shown in Fig. 5*A*, *left*. This sympathoadrenal preparation relies on the use of a platinum bipolar stimulator placed peripherally to the adrenal medulla and spanning the cortex to stimulate the splanchnic nerve prior to its entering the adrenal medulla. Bipolar stimulation took two forms. Basal stimulation was set at a constant 0.2 Hz to mimic sympathetic tone. Stress stimulation took the form of a burst protocol of four sets of 15 pulses delivered at 2 Hz with an interset interval of 15 s. Functional coupling between splanchnic nerve and chromaffin cell was determined by pacing the splanchnic nerve at a low frequency (0.05 Hz; see also "Experimental Procedures") and probing chromaffin cells in the proximal medulla with a 5-$\mu$m carbon fiber amperometry electrode to measure catecholamine secretion. Once a functional pairing was identified, we measured cumulative catecholamine release from single cells prior to and after neuronal stimulation by carbon fiber amperometry (Fig. 5*A*). We found that total catecholamine release increased under stress mode stimulation and that this increased secretion was sensitive to $Ni^{2+}$ and PKC block (Table 1). Lastly, in experiments that parallel those presented in Figs. 3 and 4, we held patch-clamped chromaffin cells in the perforated voltage clamp configuration and conducted the I-V protocol after neuronal stimulation (Fig. 5*B*). Elevated neuronal stimulation evoked a specific increase in the $Ni^{2+}$-sensitive inward current measured both at the peak potential (Fig. 5*B*, *panel i*) and at $P_{V_m}$ (Fig. 5*B*, *panel ii*), and this facilitation was blocked by PKC inhibition. Thus, augmentation of a $Ni^{2+}$-sensitive low voltage-activated conductance observed with exogenous PACAP stimulation was recapitulated under native synaptic stimulation in an activity-dependent manner.

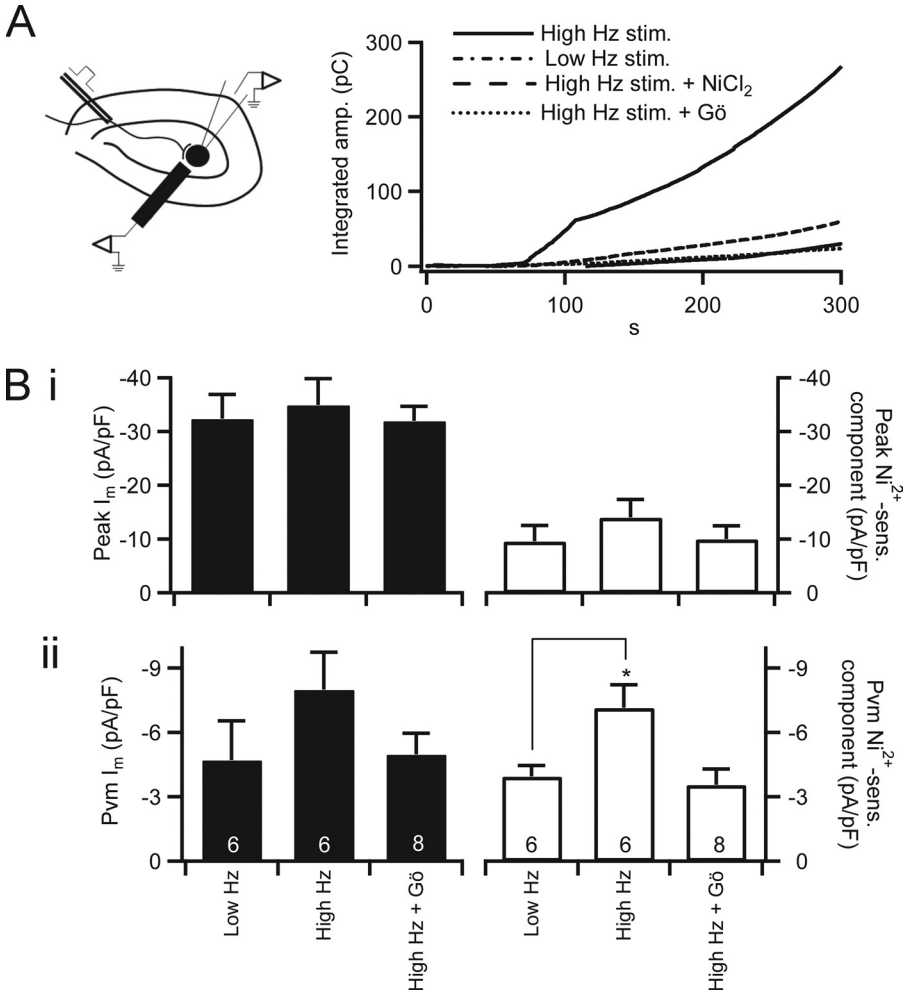


FIGURE 5. **Elevated neuronal stimulation facilitates nickel-sensitive calcium influx.** *A*, *left*, a diagram illustrates the nerve stimulation and chromaffin cell recording condition. *Right*, evoked catecholamine release was measured by carbon fiber amperometry. Total catecholamine release was determined by integrating the amperometric record as in Figs. 1 and 4. Representative traces are plotted in *B* for Low Hz stimulation (*stim.*) and High Hz stimulation in a normal Ringer's bath solution and High Hz stimulation in the presence of $Ni^{2+}$ or Gö6983-containing Ringer's bath solution. *B*, cells determined to be excitable by neuronal stimulation were patch-clamped in the perforated voltage clamp configuration after bipolar stimulation, and I-V protocols were conducted. Data are plotted as mean value, with *error bars* representing S.E. *Panel i*, peak inward (*left axis*) and the $Ni^{2+}$-sensitive (*sens.*) inward component (*right axis*) currents were measured as in Fig. 3 after bipolar neuronal stimulation with Low Hz- and High Hz-stimulated firing patterns. *Panel ii*, mean inward current at $P_{V_m}$ and the $Ni^{2+}$-sensitive component were measured in each condition as described in Fig. 4, pooled, and plotted. * indicates $p \leq 0.05$ with respect to control values determined by one-way analysis of variance. Sample size is indicated by the *number* at the *base* of each category *bar*. *pF*, picofarad; *Gö*, Gö6983.

**TABLE 1**

**Bipolar stimulation-evoked amperometric current**

Amperometric current was measured in each condition as labeled, and data were pooled. Cells were pulsed at Low Hz or High Hz stimulation. Under Low Hz stimulation, the splanchnic nerve was stimulated for 60 pulses at a frequency of 0.2 Hz. Under High Hz stimulation, the nerve was stimulated with four bursts of 15 pulses at a 2 Hz frequency with an interburst interval of 15 s. Stimuli were delivered at a constant voltage of 35 V for a 10-$\mu$s duration. Quantified pooled data were determined from baseline subtracted, integrated amperometric currents at the 60 s time point. The mean ± S.E. values are shown for each condition. Sample size is indicated in parentheses.

| Condition | Mean ± S.E. (*n*) |
|---|---|
| Low Hz stimulation | 64.4 ± 16.3 (10) |
| High Hz stimulation | 179.8 ± 41.5[a] (10) |
| High Hz stimulation + $NiCl_2$ | 51.0 ± 5.92 (8) |
| High Hz stimulation + Gö6983 | 49.5 ± 7.57 (5) |

[a] $p \leq 0.05$ with respect to control values determined by one-way analysis of variance.

## DISCUSSION

Under the basal "rest and digest" mode of energy storage set by the sympathetic tone, chromaffin cells release modest amounts of catecholamine into the circulation to regulate physiological parameters, including shunting of blood to viscera and increased insulin release. Acute stress due to external threat or injury initiates the sympathetic "fight or flight" response and causes chromaffin cells to fire at an elevated rate (66–68). This enhanced firing greatly increases the rate of catecholamine release. System-wide, catecholamine-elicited physiological responses include increased cardiac output, shunting of blood flow to skeletal muscle, generalized vasopression, increased circulating glucagon levels, and altered neuronal activity. Thus, chromaffin cells form a critical element of the acute sympathetic stress response. Previous studies have indicated that PACAP acts as a primary neurotransmitter at the splanchnic-adrenal synapse under the stress response (15–17). Indeed, PACAP-null mice have been shown to not mount a stress response to insulin shock and to perish under this challenge (17). Despite this physiologically important role, relatively little is known of how PACAP stimulation elicits the initial catecholamine burst under acute sympathetic stimulation.

Initial characterization has shown that PACAP-mediated stimulation depends on an influx of external $Ca^{2+}$ but that the cells do not fire action potentials (15, 44). We set out to investigate the cellular mechanism by which PACAP evokes calcium influx in the absence of action potential firing to achieve catecholamine release from adrenal chromaffin cells. This fundamental question was raised by the observation that PACAP stimulation acts through a requisite depolarization of the chromaffin cell to approximately −53-mV membrane potential (referred to here as the $P_{V_m}$). Blocking the depolarization by voltage clamp likewise blocked catecholamine release. However, when naïve, untreated cells were voltage-clamped to the same potential, little to no catecholamine release was observed. Thus, in addition to the depolarization to $P_{V_m}$, PACAP stimulation must act through a concurrent, second mechanism to facilitate calcium influx and persistent catecholamine release. The PACAP-evoked depolarization, catecholamine release, and facilitated LVA current occurred on a similar time scale. We conclude that PACAP-mediated adrenal excitation occurs through a dual mechanism, membrane depolarization to a level insufficient for firing of an action potential but sufficient to allow influx through LVA calcium channels and a parallel phosphodependent augmentation of LVA T-type calcium conductance.

Several key pieces of evidence demonstrate the role for a phosphorylation-mediated augmentation of T-type LVA calcium channels rather than HVA or other LVA calcium channels. First, a low voltage shoulder, a characteristic of LVA T-type channel currents (40–43, 59), was evident only after acute exposure to PACAP or stimulation with PMA or Epac activator 8-pCPT-2′-*O*-Me-cAMP (Fig. 3) and was not observed in the naïve cells or cells treated with PKC blocker. Indeed, PACAP stimulation did not significantly alter calcium influx associated with action potential excitation (Fig. 1) and if anything decreased total calcium influx under the native action potential voltage template. Thus, PACAP-dependent facilitation of calcium influx is limited to subthreshold depolarization conditions. These findings are consistent with previous studies showing that PKC activation decreases peak $Ca^{2+}$ conductance in bovine chromaffin cells (69, 70). Moreover, in rat chromaffin cells, calcium conductance through HVA L-type channels has been shown to decrease specifically after PACAP stimulation, and this effect is reversed by PKC inhibition (55). The subthreshold depolarization elicited by PACAP treatment is insufficient to activate most high voltage-activated currents. Although L-type channels exist in other tissue types with relatively low activation potentials (−40 mV) (71), we did not observe a significant PACAP effect on nifedipine-sensitive LVA conductance (data not shown).

We considered a potential contribution of R-type calcium channels in PACAP-evoked calcium entry and secretion. R-type channels are HVA calcium channels sensitive to nickel block with an initial activation potential of −40 mV (39). We selected a concentration of nickel chloride optimal for blocking T-type channels in chromaffin cells (43, 58); however, the positive activation potential of the $Ni^{2+}$-sensitive current presented in Fig. 2 indicates a component of R-type current in our $Ni^{2+}$ subtraction data. Ultimately, the depolarization evoked by PACAP was insufficient to activate HVA R-type channels; thus, any R-type contribution in our $Ni^{2+}$-sensitive current at $P_{V_m}$ would be nominal. Moreover, if this were the case, it would only mean that we are underestimating the effect of PACAP on T-type facilitation by elevating the control base line.

In the literature, there are several instances of chromaffin cell LVA T-type channel recruitment and plasticity reported mostly in response to chronic stressors. Expression of $Ca_v3.2$ is increased in adult rat chromaffin cells after 12–18 h of chronic intermittent hypoxia via a PKA-independent process (40). Similarly, Epac and $\beta$-adrenergic stimulation (on the time scale of hours) recruits T-type channels and increases T-type channel current density (59). Chronic intermittent hypoxia up-regulates $Ca_v3.1$ and $Ca_v3.2$ messages in chromaffin cells, and peak $Ni^{2+}$-sensitive current is significantly increased (42). To our knowledge, acute phosphoregulatory mechanisms of T-type calcium channels have not been studied in chromaffin cells. However, such acute regulatory mechanisms have been studied in other cell types. Several such studies report that PKC phosphorylation facilitates T-type calcium conductance (72, 73). Park *et al.* (47) found that PKC phosphorylation increases peak T-type current amplitude when expressed in *Xenopus* oocytes. However, this facilitation was not related to an increase in channel surface density. They propose that PKC phosphorylation converts non-functional or latent T-type channels to functional conductive forms. Consistent with this finding, we demonstrated a significant expression of $Ca_v3.2$ in naïve chromaffin cells but measurable LVA current only after PKC activation. We were not able to discern whether the immunoreactivity demonstrated in Fig. 2 is surface or internal. Despite this point, we did demonstrate that PKC activity recruited T-type $Ca_v3.2$ calcium channels to a functional conductive form during the acute stress response.

Our data demonstrate that direct neuronal stimulation designed to mimic burst mode sympathetic firing elicited catecholamine release that was sensitive to $Ni^{2+}$, and evoked a facilitation of LVA $Ca^{2+}$ conductance. We conclude that native PACAP stimulation resulted from the combined effects of a subthreshold depolarization and a potential sufficient to trigger LVA calcium channel opening. In a parallel effect, PACAP stimulation led to a protein kinase C-dependent phosphoregulated facilitation of T-type calcium influx.

*Acknowledgments—We thank Dr. Katherine Trueblood, Prattana Samasilp, and Dr. Bryan Doreian for technical assistance in the RT-quantitative PCR detection of LVA channel message.*

## REFERENCES

1. Aunis, D. (1998) *Int. Rev. Cytol.* **181,** 213–320
2. Albillos, A., Neher, E., and Moser, T. (2000) *J. Neurosci.* **20,** 8323–8330
3. Chan, S. A., Polo-Parada, L., and Smith, C. (2005) *Arch. Biochem. Biophys.* **435,** 65–73
4. *García*, A. G., *García*-De-Diego, A. M., *Gandía*, L., Borges, R., and *García*-Sancho, J. (2006) *Physiol. Rev.* **86,** 1093–1131
5. Carmichael, S. W., and Winkler, H. (1985) *Sci. Am.* **253,** 40–49
6. Klevans, L. R., and Gebber, G. L. (1970) *J. Pharmacol. Exp. Ther.* **172,** 69–76
7. Bevington, A., and Radda, G. K. (1985) *Biochem. Pharmacol.* **34,** 1497–1500

8. Boksa, P., and Livett, B. G. (1984) *J. Neurochem.* **42,** 618–627
9. Marley, P. D. (1988) *Trends Pharmacol. Sci.* **9,** 102–107
10. McFadden, P. N., and Koshland, D. E., Jr. (1990) *Proc. Natl. Acad. Sci. U.S.A.* **87,** 2031–2035
11. Sala, F., Nistri, A., and Criado, M. (2008) *Acta Physiol.* **192,** 203–212
12. Currie, K. P., and Fox, A. P. (1997) *J. Neurosci.* **17,** 4570–4579
13. Henry, J. P. (1992) *Integr. Physiol. Behav. Sci.* **27,** 66–83
14. Wakade, A. R. (1998) *Adv. Pharmacol.* **42,** 595–598
15. Przywara, D. A., Guo, X., Angelilli, M. L., Wakade, T. D., and Wakade, A. R. (1996) *J. Biol. Chem.* **271,** 10545–10550
16. Kuri, B. A., Chan, S. A., and Smith, C. B. (2009) *J. Neurochem.* **110,** 1214–1225
17. Hamelink, C., Tjurmina, O., Damadzic, R., Young, W. S., Weihe, E., Lee, H. W., and Eiden, L. E. (2002) *Proc. Natl. Acad. Sci. U.S.A.* **99,** 461–466
18. Braas, K. M., Brandenburg, C. A., and May, V. (1994) *Endocrinology* **134,** 186–195
19. Hoshino, M., Li, M., Zheng, L. Q., Suzuki, M., Mochizuki, T., and Yanaihara, N. (1993) *Neurosci. Lett.* **159,** 35–38
20. Tischler, A. S., Riseberg, J. C., and Gray, R. (1995) *Neurosci. Lett.* **189,** 135–138
21. Hamelink, C., Lee, H. W., Chen, Y., Grimaldi, M., and Eiden, L. E. (2002) *J. Neurosci.* **22,** 5310–5320
22. Guo, X., and Wakade, A. R. (1994) *J. Physiol.* **475,** 539–545
23. Watanabe, T., Masuo, Y., Matsumoto, H., Suzuki, N., Ohtaki, T., Masuda, Y., Kitada, C., Tsuda, M., and Fujino, M. (1992) *Biochem. Biophys. Res. Commun.* **182,** 403–411
24. Hagen, B. M., Bayguinov, O., and Sanders, K. M. (2006) *Am. J. Physiol. Cell Physiol.* **291,** C375–C385
25. Montero-Hadjadje, M., Delarue, C., Fournier, A., Vaudry, H., and Yon, L. (2006) *Ann. N.Y. Acad. Sci.* **1070,** 431–435
26. Gerdin, M. J., and Eiden, L. E. (2007) *Sci. STKE* **2007,** pe15
27. Ster, J., de Bock, F., Bertaso, F., Abitbol, K., Daniel, H., Bockaert, J., and Fagni, L. (2009) *J. Physiol.* **587,** 101–113
28. Mustafa, T., Grimaldi, M., and Eiden, L. E. (2007) *J. Biol. Chem.* **282,** 8079–8091
29. Morita, K., Sakakibara, A., Kitayama, S., Kumagai, K., Tanne, K., and Dohi, T. (2002) *J. Pharmacol. Exp. Ther.* **302,** 972–982
30. Watanabe, T., Shimamoto, N., Takahashi, A., and Fujino, M. (1995) *Am. J. Physiol. Endocrinol. Metab.* **269,** E903–E909
31. Maturana, A., Lenglet, S., Python, M., Kuroda, S., and Rossier, M. F. (2009) *Endocrinology* **150,** 3726–3734
32. Braun, M., Ramracheya, R., Bengtsson, M., Zhang, Q., Karanauskaite, J., Partridge, C., Johnson, P. R., and Rorsman, P. (2008) *Diabetes* **57,** 1618–1628
33. Dreyfus, F. M., Tscherter, A., Errington, A. C., Renger, J. J., Shin, H. S., Uebele, V. N., Crunelli, V., Lambert, R. C., and Leresche, N. (2010) *J. Neurosci.* **30,** 99–109
34. Ono, K., and Iijima, T. (2010) *J. Mol. Cell. Cardiol.* **48,** 65–70
35. Zamponi, G. W., Lory, P., and Perez-Reyes, E. (2010) *Pflugers Arch.* **460,** 395–403
36. Perez-Reyes, E. (2003) *Physiol. Rev.* **83,** 117–161
37. Carbone, E., Giancippoli, A., Marcantoni, A., Guido, D., and Carabelli, V. (2006) *Cell Calcium* **40,** 147–154
38. Marcantoni, A., Carabelli, V., Comunanza, V., Hoddah, H., and Carbone, E. (2008) *Acta Physiol.* **192,** 233–246
39. Randall, A. D., and Tsien, R. W. (1997) *Neuropharmacology* **36,** 879–893
40. Carabelli, V., Marcantoni, A., Comunanza, V., de Luca, A., Díaz, J., Borges, R., and Carbone, E. (2007) *J. Physiol.* **584,** 149–165
41. Giancippoli, A., Novara, M., de Luca, A., Baldelli, P., Marcantoni, A., Carbone, E., and Carabelli, V. (2006) *Biophys. J.* **90,** 1830–1841
42. Souvannakitti, D., Nanduri, J., Yuan, G., Kumar, G. K., Fox, A. P., and Prabhakar, N. R. (2010) *J. Neurosci.* **30,** 10763–10772
43. Levitsky, K. L., and López-Barneo, J. (2009) *J. Physiol.* **587,** 1917–1929
44. Taupenot, L., Mahata, M., Mahata, S. K., and O'Connor, D. T. (1999) *Hypertension* **34,** 1152–1162
45. Tanaka, K., Shibuya, I., Harayama, N., Nomura, M., Kabashima, N., Ueta, Y., and Yamashita, H. (1997) *Endocrinology* **138,** 4086–4095
46. Zhou, C. J., Yada, T., Kohno, D., Kikuyama, S., Suzuki, R., Mizushima, H., and Shioda, S. (2001) *Peptides* **22,** 1111–1117
47. Park, J. Y., Kang, H. W., Moon, H. J., Huh, S. U., Jeong, S. W., Soldatov, N. M., and Lee, J. H. (2006) *J. Physiol.* **577,** 513–523
48. Walz, W., Boulton, A., and Baker, G. (eds) (2002) *Patch-Clamp Analysis: Advanced Techniques*, Vol. 35, p. 163, Humana Press, Totowa, NJ
49. Chan, S. A., and Smith, C. (2003) *J. Physiol.* **553,** 707–717
50. Burgoyne, R. D. (1995) *Pflugers Arch.* **430,** 213–219
51. Smith, C., and Neher, E. (1997) *J. Cell Biol.* **139,** 885–894
52. Tanaka, K., Shibuya, I., Nagamoto, T., Yamashita, H., and Kanno, T. (1996) *Endocrinology* **137,** 956–966
53. Geng, G., Gaspo, R., Trabelsi, F., and Yamaguchi, N. (1997) *Am. J. Physiol. Regul. Integr. Comp. Physiol.* **273,** R1339–R1345
54. Hayashi, K., Endoh, T., Shibukawa, Y., Yamamoto, T., and Suzuki, T. (2002) *Bull. Tokyo Dent. Coll.* **43,** 31–39
55. Jorgensen, M. S., Liu, J., Adams, J. M., Titlow, W. B., and Jackson, B. A. (2002) *Regul. Pept.* **103,** 59–65
56. Perez-Reyes, E. (1998) *J. Bioenerg. Biomembr.* **30,** 313–318
57. Kang, H. W., Park, J. Y., Jeong, S. W., Kim, J. A., Moon, H. J., Perez-Reyes, E., and Lee, J. H. (2006) *J. Biol. Chem.* **281,** 4823–4830
58. Carabelli, V., Marcantoni, A., Comunanza, V., and Carbone, E. (2007) *Eur. Biophys. J.* **36,** 753–762
59. Novara, M., Baldelli, P., Cavallari, D., Carabelli, V., Giancippoli, A., and Carbone, E. (2004) *J. Physiol.* **558,** 433–449
60. Turquier, V., Yon, L., Grumolato, L., Alexandre, D., Fournier, A., Vaudry, H., and Anouar, Y. (2001) *Mol. Pharmacol.* **60,** 42–52
61. Hucho, T. B., Dina, O. A., and Levine, J. D. (2005) *J. Neurosci.* **25,** 6119–6126
62. Holz, G. G., Kang, G., Harbeck, M., Roe, M. W., and Chepurny, O. G. (2006) *J. Physiol.* **577,** 5–15
63. Kang, G., Joseph, J. W., Chepurny, O. G., Monaco, M., Wheeler, M. B., Bos, J. L., Schwede, F., Genieser, H. G., and Holz, G. G. (2003) *J. Biol. Chem.* **278,** 8279–8285
64. Fenwick, E. M., Marty, A., and Neher, E. (1982) *J. Physiol.* **331,** 577–597
65. Florey, C. D. (1993) *BMJ* **306,** 1181–1184
66. Brandt, B. L., Hagiwara, S., Kidokoro, Y., and Miyazaki, S. (1976) *J. Physiol.* **263,** 417–439
67. Holman, M. E., Coleman, H. A., Tonta, M. A., and Parkington, H. C. (1994) *J. Physiol.* **478,** 115–124
68. Kidokoro, Y., and Ritchie, A. K. (1980) *J. Physiol.* **307,** 199–216
69. Gillis, K. D., Mossner, R., and Neher, E. (1996) *Neuron* **16,** 1209–1220
70. Smith, C. (1999) *J. Neurosci.* **19,** 589–598
71. Lipscombe, D., Helton, T. D., and Xu, W. (2004) *J. Neurophysiol.* **92,** 2633–2641
72. Furukawa, T., Ito, H., Nitta, J., Tsujino, M., Adachi, S., Hiroe, M., Marumo, F., Sawanobori, T., and Hiraoka, M. (1992) *Circ. Res.* **71,** 1242–1253
73. Joksovic, P. M., Choe, W. J., Nelson, M. T., Orestes, P., Brimelow, B. C., and Todorovic, S. M. (2010) *Mol. Pharmacol.* **77,** 87–94